On Resolution-of-the-Identity Electron Repulsion Integral Approximations and Variational Stability

Lukas N. Wirz, Simen S. Reine, and Thomas Bondo Pedersen*

Hylleraas Centre for Quantum Molecular Sciences, Department of Chemistry, University of Oslo, P.O. Box 1033 Blindern, N-0315 Oslo, Norway

E-mail: t.b.pedersen@kjemi.uio.no

Abstract

The definiteness of the Mulliken and Dirac electron repulsion integral (ERI) matrices is examined for different classes of resolution-of-the-identity (RI) ERI approximations with particular focus on local fitting techniques. For global RI, robust local RI, and nonrobust local RI we discuss the definiteness of the approximated ERI matrices as well as the resulting bounds of Hartree, exchange, and total energies. Lower bounds of Hartree and exchange energy contributions are crucial as their absence may lead to variational instabilities, causing severe convergence problems or even convergence to a spurious state in self-consistent-field optimizations. While the global RI approximation guarantees lower bounds of Hartree and exchange energies, local RI approximations are generally unbounded. The robust local RI approximation guarantees a lower bound of the exchange energy but not of the Hartree energy. The nonrobust local RI approximation guarantees a lower bound of the Hartree energy but not of the exchange energy. These issues are demonstrated by sample calculations on carbon dioxide and benzene using the pair atomic RI approximation.

1 Introduction

Solving the electronic Schrödinger equation of molecular system within the clamped-nucleus Born-Oppenheimer approximation is a central problem in quantum chemistry. Variational optimization of an approximate wave function is possible since the eigenvalues of the Hamiltonian are bounded from below on the Sobolev space of admissible wave functions.[1] This indicates a delicate balance between the total kinetic energy and the total potential (Coulombic electron–nucleus attraction and electron–electron repulsion) energy and, indeed, it can be shown that the potential energy is bounded from above by the kinetic energy.[1]

In practical computational models using expansions in local atom-centered one-electron basis functions, whether analytical or numerical, the electron-electron interactions are described by means of electron repulsion integrals (ERIs) and insisting on a numerically exact treatment of ERIs would prevent studies of all but the smallest systems. To accelerate calculations the ERIs are approximated, either by prescreening techniques designed to avoid calculation of ERIs that contribute insignificantly to the quantity of interest, or by more drastic approximations that replace some or all ERIs with less computationally demanding expressions. Modern examples include prescreening based on integral estimates,[2–7] resolution-of-the-identity (RI, also called density fitting, DF) approximations,[8–44] pseudospectral and seminumerical integration methods,[45–51] and tensor decomposition techniques.[52–66]

Introducing the limited expansion of diatomic overlap (LEDO) approximation,[67] Billingsley and Bloor formulated four criteria that an acceptable ERI approximation should satisfy: (1) formal applicability to any atomic orbital (AO) basis set, (2) invariance to rotation of the molecular coordinate system, (3) reliable behavior within reasonable ranges of such parameters as orbital exponents and geometry, and (4) at least an order of magnitude faster than exact calculation. A fifth criterion, guaranteed variational stability, may be obvious but appears to be overlooked in the literature.

Merlot et al.[38] proved theoretically that local RI approximations combined with Dunlap's robust fitting scheme[14,20,21,37] lead to Hartree energies without a rigorous lower bound

and thus to potential variational collapse, and demonstrated computationally that the most radical local RI scheme, the pair-atomic RI (PARI) approximation, indeed shows variational instability. Although variational collapse is relatively rare within the PARI approximation, occurring in about 1% of the predominantly organic molecules tested,[38,40] this clearly is an unfortunate property of any ERI approximation. In an attempt to circumvent variational instability issues, Ihrig et al.[43] used the nonrobust PARI approximation with large automatically generated auxiliary basis sets to offset the concomitant reduction of accuracy, showing that reasonable accuracy is achieved not only for the Hartree contribution but also for the exact exchange and correlation contributions. The implementation of Ihrig et al. is based on numerical AOs and it seems natural to adapt their auxiliary basis set generation scheme, which can be viewed as an extension of the atomic Cholesky decomposition (aCD) approach,[68,69] to Gaussian-type orbitals. In this work, we present a theoretical analysis of variational stability within RI approximations and use a Gaussian adaptation of the auxiliary basis set generation of Ihrig et al. to illustrate our findings computationally.

2 Theory

2.1 General properties of electron repulsion energies

Before analyzing effects of ERI approximations on variational stability, we first recapitulate some well-known properties of exact ERIs and electron repulsion energies. We assume that an orthonormal set of spin orbitals have been chosen such that the second-quantization Coulombic two-electron operator can be written as (see, e.g., Helgaker et al.[70])

$$\hat{G} = \frac{1}{2} \sum_{pqrs} \langle pq|rs\rangle a_p^\dagger a_q^\dagger a_s a_r \tag{1}$$

where $a_p^\dagger$ and a_p are creation and annihilation operators corresponding to the spin orbitals and satisfying the anticommutation relations $[a_p^\dagger, a_q]_+ = \delta_{pq}$ and $[a_p^\dagger, a_q^\dagger]_+ = [a_p, a_q]_+ = 0$.

We have used Dirac notation for the ERIs in spin-orbital basis,

$$\langle pq|rs\rangle = \iint \psi_p(\boldsymbol{x}_1)^* \psi_q(\boldsymbol{x}_2)^* r_{12}^{-1} \psi_r(\boldsymbol{x}_1) \psi_s(\boldsymbol{x}_2) \mathrm{d}\boldsymbol{x}_1 \mathrm{d}\boldsymbol{x}_2 \tag{2}$$

where the integrations are over combined spin and space variables $\boldsymbol{x}_i = (\boldsymbol{r}_i, \xi_i)$ and $r_{12} = |\boldsymbol{r}_1 - \boldsymbol{r}_2|$.

The electron repulsion energy in an arbitrary state $|\Psi\rangle$ in Fock space is expressed in terms of the ERIs and the Hermitian two-electron density matrix $d_{pq,rs} = \langle \Psi | a_p^\dagger a_q^\dagger a_s a_r | \Psi \rangle$, which is easily shown to be positive semidefinite

$$\sum_{pqrs} v_{pq}^* d_{pq,rs} v_{rs} = \langle \Psi_v | \Psi_v \rangle \geq 0 \tag{3}$$

where $\boldsymbol{v}$ is a complex vector and $|\Psi_v\rangle = \sum_{pq} v_{pq} a_q a_p |\Psi\rangle$. Hence, the two-electron density matrix may be Cholesky decomposed, $d_{pq,rs} = \sum_J L_{pq,J}^* L_{rs,J}$, and the electron repulsion energy can be written as

$$\langle \Psi | \hat{G} | \Psi \rangle = \frac{1}{2} \sum_J \sum_{pqrs} L_{pq,J}^* \langle pq|rs\rangle L_{rs,J} \tag{4}$$

Each term in the J-sum is nonnegative if and only if the Dirac ERIs form a Hermitian positive semidefinite matrix. Noting that the Coulomb operator r_{12}^{-1} is nonnegative, this is easily verified:

$$\sum_{pqrs} v_{pq}^* \langle pq|rs\rangle v_{rs} = \iint r_{12}^{-1} |f_v(\boldsymbol{x}_1, \boldsymbol{x}_2)|^2 \mathrm{d}\boldsymbol{x}_1 \mathrm{d}\boldsymbol{x}_2 \geq 0 \tag{5}$$

where $\boldsymbol{v}$ is a complex vector and $f_v(\boldsymbol{x}_1, \boldsymbol{x}_2) = \sum_{pq} v_{pq} \psi_p(\boldsymbol{x}_1) \psi_q(\boldsymbol{x}_2)$. Consequently, the electron repulsion energy is bounded from below

$$\langle \Psi | \hat{G} | \Psi \rangle \geq 0 \tag{6}$$

We thus have demonstrated the intuitively obvious result: the electron repulsion energy is

nonnegative in any (exact or approximate) state. Clearly, nonnegativity is guaranteed only if the Dirac ERI matrix is positive semidefinite, placing a rather severe constraint on ERI approximations designed to accelerate computations.

It is important, however, to distinguish between variational instability and negative electron repulsion energy. Variational stability is guaranteed as long as the electron repulsion energy is bounded from below, even if the greatest lower bound is negative (and finite). Of course, a negative electron repulsion energy indicates that the electron-electron interaction is, effectively, attractive and hence unphysical, but it does not in itself indicate variational collapse.

For the important special case of a single-determinant state $|\Psi\rangle$, the electron repulsion energy can be written as the sum of the Hartree energy, E_H, and the exchange energy, E_x,

$$E = \langle\Psi|\hat{G}|\Psi\rangle = E_H + E_x, \qquad E_H = \frac{1}{2}\sum_{ij}\langle ij|ij\rangle, \qquad E_x = -\frac{1}{2}\sum_{ij}\langle ij|ji\rangle \tag{7}$$

where i, j refer to spin orbitals that are occupied in $|\Psi\rangle$. Slater[71] (see also Roothaan,[72] Whitten,[9] and Power and Pitzer[73]) used Poisson's equation and Green's theorem to show that for any function $f(\boldsymbol{r})$ decaying sufficiently rapidly as $|\boldsymbol{r}| \to \infty$ we have

$$\iint f(\boldsymbol{r}_1)^* r_{12}^{-1} f(\boldsymbol{r}_2) \mathrm{d}\boldsymbol{r}_1 \mathrm{d}\boldsymbol{r}_2 \geq 0 \tag{8}$$

It follows from this inequality that the Hartree energy is nonnegative, $E_H \geq 0$. The exchange energy is easily shown to be nonpositive,

$$E_x = -\frac{1}{2}\iint r_{12}^{-1} |\rho(\boldsymbol{x}_1, \boldsymbol{x}_2)|^2 \mathrm{d}\boldsymbol{x}_1 \mathrm{d}\boldsymbol{x}_2 \leq 0 \tag{9}$$

where $\rho(\boldsymbol{x}_1, \boldsymbol{x}_2) = \sum_i \psi_i(\boldsymbol{x}_1)^* \psi_i(\boldsymbol{x}_2)$. Since the total electron repulsion energy is nonnegative,

the Hartree energy must be greater than the absolute value of the exchange energy, i.e.

$$E_H \geq -E_x \geq 0 \tag{10}$$

This relation ensures variational stability of Hartree-Fock (HF) theory.

Roothaan[72] obtained this result by proving a stronger inequality relating the individual integrals $\langle ij|ij\rangle$ and $\langle ij|ji\rangle$, which are both real and nonnegative. Following Roothaan,[72] we note that the positive semidefiniteness of the Dirac ERI matrix implies $\langle ij - ji|ij - ji\rangle \geq 0$ and thus

$$\langle ij|ij\rangle \geq \langle ij|ji\rangle \geq 0 \tag{11}$$

from which inequality (10) follows immediately.

2.2 RI approximation

The perhaps most widespread approach to accelerate electronic structure calculations using atom-centered basis functions is the RI approximation to ERIs. The RI approach does not aim directly at the Dirac ERI matrix. Rather, it exploits the rank deficiency of the Mulliken ERI matrix in AO basis,

$$(ab|cd) = \iint a(\boldsymbol{r}_1)b(\boldsymbol{r}_1)r_{12}^{-1}c(\boldsymbol{r}_2)d(\boldsymbol{r}_2)\mathrm{d}\boldsymbol{r}_1\mathrm{d}\boldsymbol{r}_2 \tag{12}$$

where a, b, c, d denote AOs, which we assume real. It follows from Slater's result (8) that the Mulliken ERI matrix is symmetric positive semidefinite,

$$\sum_{abcd} v_{ab}(ab|cd)v_{cd} = (f_v|f_v) \geq 0 \tag{13}$$

where $f_v(\boldsymbol{r}) = \sum_{ab} v_{ab}a(\boldsymbol{r})b(\boldsymbol{r})$ with v_{ab} real.

Employing an auxiliary basis set $\{\alpha(\boldsymbol{r})\}$, usually chosen to be atom-centered, the basic

idea of the RI approach is to fit the AO products according to

$$|ab) \approx |\widetilde{ab}) = \sum_{\alpha} |\alpha) C_{\alpha}^{ab} \tag{14}$$

Introducing the Coulomb-metric fitting error $|\Delta_{ab}) = |ab - \widetilde{ab})$, the identity

$$(ab|cd) = (\widetilde{ab}|\widetilde{cd}) + (\widetilde{ab}|\Delta_{cd}) + (\Delta_{ab}|\widetilde{cd}) + (\Delta_{ab}|\Delta_{cd}) \tag{15}$$

is readily obtained. Determining the fitting coefficients $\boldsymbol{C}$ by variational minimization of the Coulomb-metric norm of the individual fitting errors,

$$\tau_{ab}^2 = (\Delta_{ab}|\Delta_{ab}) \tag{16}$$

we obtain the rather obvious requirement that the fitting error must belong to the orthogonal complement of the space spanned by the auxiliary functions. That is, $(\alpha|\Delta_{ab}) = 0$, which may be recast as the linear fitting equations

$$\sum_{\beta} (\alpha|\beta) C_{\beta}^{ab} = (\alpha|ab) \tag{17}$$

The terms linear in the fitting error thus vanish in Eq. (15) and the RI approximation to the ERIs,

$$(ab|cd) \approx \widetilde{(ab|cd)} = (\widetilde{ab}|\widetilde{cd}) \tag{18}$$

becomes bilinear in the fitting errors:

$$|(ab|cd) - (\widetilde{ab}|\widetilde{cd})| = |(\Delta_{ab}|\Delta_{cd})| \leq \tau_{ab}\tau_{cd} \tag{19}$$

The fitting error norms τ_{ab} can be made arbitrarily small by a suitable choice of auxiliary basis set, and the overall accuracy of the RI approximation may thus be controlled.

While the RI Mulliken ERI matrix is symmetric positive semidefinite

$$\sum_{abcd} v_{ab}\widetilde{(ab|cd)}v_{cd} = \sum_{abcd} v_{ab}(\widetilde{ab}|\widetilde{cd})v_{cd} = (\tilde{f}_v|\tilde{f}_v) \geq 0 \tag{20}$$

where $\tilde{f}_v(\boldsymbol{r}) = \sum_\alpha [\sum_{ab} v_{ab} C_\alpha^{ab}]\alpha(\boldsymbol{r})$, the RI Dirac ERI matrix is symmetric indefinite

$$\sum_{abcd} v_{ab}\widetilde{\langle ab|cd\rangle}v_{cd} = \sum_{abcd} v_{ab}\widetilde{(ac|bd)}v_{cd} = \sum_{ab}(X_{ab}|\bar{X}_{ba}) \tag{21}$$

$$X_{ab}(\boldsymbol{r}) = \sum_\alpha \left[\sum_c C_\alpha^{ac} v_{cb}\right] \alpha(\boldsymbol{r}), \qquad \bar{X}_{ba}(\boldsymbol{r}) = \sum_\alpha \left[\sum_c C_\alpha^{bc} v_{ac}\right] \alpha(\boldsymbol{r}) \tag{22}$$

This implies that, for a general electronic state, the total electron repulsion energy may be negative within the RI approximation, which thus threatens variational stability unless a lower bound can be established. The indefiniteness can be seen more clearly by considering the RI approach an explicit approximation of the Coulomb operator,

$$r_{12}^{-1} \approx \sum_J \phi_J(\boldsymbol{r}_1)\phi_J(\boldsymbol{r}_2) \tag{23}$$

Here we have introduced the auxiliary potentials

$$\phi_J(\boldsymbol{r}) = \int \frac{\sum_\alpha \alpha(\boldsymbol{r}')L_\alpha^J}{|\boldsymbol{r} - \boldsymbol{r}'|}\mathrm{d}\boldsymbol{r}' \tag{24}$$

and the Cholesky decomposed inverse metric matrix

$$(\alpha|\beta)^{-1} = \sum_J L_\alpha^J L_\beta^J \tag{25}$$

where the common short-hand notation $(\alpha|\beta)^{-1}$ is used for the α, β element of the inverse of the metric matrix with elements $(\alpha|\beta)$. The RI approximation to the ERIs may then be

written in terms of overlap integrals,

$$(ab|cd) \approx (\widetilde{ab}|\widetilde{cd}) = \left[\int a(\boldsymbol{r})b(\boldsymbol{r})\phi_J(\boldsymbol{r})\mathrm{d}\boldsymbol{r}\right]\left[\int \phi_J(\boldsymbol{r})c(\boldsymbol{r})d(\boldsymbol{r})\mathrm{d}\boldsymbol{r}\right] \tag{26}$$

which paves the way for a Poisson-basis formulation of RI.[74] Evidently, the RI Coulomb operator, Eq. (23), is not generally positive and integrals of the form

$$I_J = \iint f(\boldsymbol{r}_1,\boldsymbol{r}_2)^2\phi_J(\boldsymbol{r}_1)\phi_J(\boldsymbol{r}_2)\mathrm{d}\boldsymbol{r}_1\mathrm{d}\boldsymbol{r}_2 \tag{27}$$

may be negative, implying that the RI Dirac ERI matrix is not positive semidefinite in general.

We now turn to the important case of a closed-shell single-determinant state. The RI Hartree energy is nonnegative

$$\tilde{E}_H = \frac{1}{2}\sum_{abcd} D_{ab}(\widetilde{ab}|\widetilde{cd})D_{cd} \geq 0 \tag{28}$$

where $\boldsymbol{D}$ is the density matrix in AO basis. Furthermore,

$$\Delta\tilde{E}_H = E_H - \tilde{E}_H = \frac{1}{2}\sum_{abcd} D_{ab}(\Delta_{ab}|\Delta_{cd})D_{cd} \geq 0 \tag{29}$$

and hence the RI Hartree energy is bounded both from above and from below

$$0 \leq \tilde{E}_H \leq E_H \tag{30}$$

The RI exchange energy is nonpositive

$$\tilde{E}_x = -\frac{1}{4}\sum_{abcd} D_{ab}(\widetilde{ac}|\widetilde{bd})D_{cd} = -\frac{1}{4}\sum_{ij}(\widetilde{ij}|\widetilde{ij}) \leq 0 \tag{31}$$

where i, j refer to occupied molecular orbitals (MOs) obtained, for instance, from Cholesky

decomposition of the positive semidefinite density matrix $\boldsymbol{D}$[75] or by diagonalization of the Fock matrix. Furthermore,

$$\Delta\tilde{E}_x = E_x - \tilde{E}_x = -\frac{1}{4}\sum_{abcd} D_{ab}(\Delta_{ac}|\Delta_{bd})D_{cd} = -\frac{1}{4}\sum_{ij}(\Delta_{ij}|\Delta_{ij}) \leq 0 \tag{32}$$

and hence also the RI exchange energy is bounded both from above and from below

$$E_x \leq \tilde{E}_x \leq 0 \tag{33}$$

With $E_H = \tilde{E}_H + \Delta\tilde{E}_H$ and $E_x = \tilde{E}_x + \Delta\tilde{E}_x$, Eq. (10) can be recast as

$$\tilde{E}_H + \tilde{E}_x \geq -\left(\Delta\tilde{E}_H + \Delta\tilde{E}_x\right) \tag{34}$$

which shows that a single-determinant state may exist for which the total RI electron repulsion energy is negative. This, however, does not imply that the RI approximation leads to variational instability, since both $\tilde{E}_H$ and $\tilde{E}_x$ are bounded from below. Moreover, using the same auxiliary basis for both contributions and recalling that $\Delta\tilde{E}_H$ and $\Delta\tilde{E}_x$ are oppositely signed quantities, one expects substantial error cancellation so that the right-hand side of Eq. (34) is close to zero.

The fitting equations (17) ensure that the integral errors are minimized and, using a carefully designed auxiliary basis set, we can easily make the errors of the RI Hartree and exchange energies small enough that the positivity of total electron repulsion energy is guaranteed in practice. Indeed, we are not aware of any published examples of negative electron repulsion energies caused by the RI approximation. Auxiliary basis sets have been optimized for Hartree and exchange energies by, e.g., Weigend.[22,76,77] An alternative approach is to use the aCD procedure to automatically generate an auxiliary basis set with tunable accuracy[68,69] and wider applicability.[78–80]

2.3 Local RI approximations

Local RI approximations can be roughly divided into three main categories, local domain fitting, local metric fitting, and combinations of the two. The common idea is to explicitly and/or implicitly curb the long-range decay[26,27] of the fitting coefficients, by limiting the auxiliary basis expansion to functions in the neighborhood of the target product (local domain fitting) and/or by using a local metric to quench contributions from distant auxiliary functions (local metric fitting).

For our present purposes the details of the local fitting procedure are not important. The crucial point is that the linear equations (17) for a given AO product ab are not satisfied for all auxiliary functions, i.e. $(\alpha|\Delta_{ab}) \neq 0$ for some or, in the case of local metric fitting, all auxiliary functions. The identities (15) and

$$(ab|cd) = (\widetilde{ab}|cd) + (ab|\widetilde{cd}) - (\widetilde{ab}|\widetilde{cd}) + (\Delta_{ab}|\Delta_{cd}) \tag{35}$$

point to two different ERI approximations. The nonrobust ERI approximation

$$(ab|cd) \approx \widetilde{(ab|cd)}_{\mathrm{nr}} = (\widetilde{ab}|\widetilde{cd}) \tag{36}$$

leads to ERI errors linear in the fitting error, while Dunlap's robust ERI approximation[14,20,21,37]

$$(ab|cd) \approx \widetilde{(ab|cd)}_{\mathrm{r}} = (ab|\widetilde{cd}) + (\widetilde{ab}|cd) - (\widetilde{ab}|\widetilde{cd}) \tag{37}$$

shows bilinear errors. Neither of these expressions leads to a positive semidefinite Dirac ERI matrix, implying that total electron repulsion energies are not manifestly nonnegative.

The nonrobust ERI expression gives a positive semidefinite Mulliken ERI matrix, implying that the nonrobust Hartree energy is nonnegative

$$\tilde{E}_H^{\mathrm{nr}} = \frac{1}{2} \sum_{abcd} D_{ab} \widetilde{(ab|cd)}_{\mathrm{nr}} D_{cd} \geq 0 \tag{38}$$

and hence bounded from below. Since the Mulliken ERI error matrix, $(ab|cd) - \widetilde{(ab|cd)}_{\mathrm{nr}}$, is symmetric indefinite by Eq. (15), the nonrobust Hartree energy is not bounded from above by the exact Hartree energy for a given single-determinant state. Analogously, the nonrobust exchange energy is nonpositive,

$$\tilde{E}_x^{\mathrm{nr}} = -\frac{1}{4}\sum_{abcd} D_{ab}\widetilde{(ac|bd)}_{\mathrm{nr}} D_{cd} = -\frac{1}{4}\sum_{ij}(\widetilde{ij}|\widetilde{ij}) \leq 0 \tag{39}$$

and hence bounded from above, but unbounded from below by Eq. (15). This implies that the nonrobust total electron repulsion energy may become negative and even variationally unstable. Note that variational instability solely arises from the nonrobust exchange contribution.

The robust ERI expression gives an indefinite Mulliken ERI matrix, implying that the robust Hartree energy is not bounded from below.[38] It is, however, bounded from above by the exact Hartree energy for a given single-determinant state,

$$E_H - \tilde{E}_H^{\mathrm{r}} = \frac{1}{2}\sum_{abcd} D_{ab}(\Delta_{ab}|\Delta_{cd}) D_{cd} \geq 0 \tag{40}$$

The robust exchange energy is not bounded from above, i.e. it may become positive, but bounded from below,[41]

$$E_x - \tilde{E}_x^{\mathrm{r}} = -\frac{1}{4}\sum_{abcd} D_{ab}(\Delta_{ac}|\Delta_{bd}) D_{cd} = -\frac{1}{4}\sum_{abcd}(\Delta_{ij}|\Delta_{ij}) \leq 0 \tag{41}$$

Consequently, the robust electron repulsion energy is not bounded from below and robust local RI thus is variationally unstable in general. In contrast to nonrobust local RI, however, the instability solely arises from the Hartree contribution.

Manzer et al.[41] showed that the robust exchange energy is in fact bounded from below by the RI exchange energy, i.e.

$$\tilde{E}_x^{\mathrm{r}} \geq \tilde{E}_x \geq E_x \tag{42}$$

The combination of (global) RI or nonrobust local RI for the Hartree contribution and robust local RI for the exchange contribution thus is not expected to present stability issues in practice, but may yield negative electron repulsion energies.

3 Computational investigation

3.1 Automatic generation of auxiliary basis sets

The PARI approximation, in which products of two AOs a and b are expanded using auxiliary functions located on the two centers, is the most extreme case of robust local RI.[38] With the nonrobust PARI (NRPARI) approximation, the calculation of three-center integrals is avoided at the expense of energy errors that are linear in the fitting error, implying a significantly reduced accuracy. These increased errors must be compensated by using larger customized auxiliary basis sets, which ideally include explicitly the product space of the regular basis set.

Inspired by the generation of numerical auxiliary bases proposed by Ihrig et al.,[43] we have computed atom-centered auxiliary Gaussian basis sets for use in nonrobust local RI through a modification of the aCD scheme.[68,69] The auxiliary basis set is automatically generated for each atom based on the employed regular basis set $\{a\}$ centered on that atom. In a first optional step, functions $\{x\}$ are added with higher angular momentum or smaller exponents than the functions in $\{a\}$, forming the extended basis $\{a\}\cup\{x\}$. The complete product space $\{p\}$ is built according to $\{p\} = (\{a\} \cup \{x\}) \otimes (\{a\} \cup \{x\})$. One may choose to decontract $\{a\}$ before building the product space. The matrix of integrals $(p|p)$ is then constructed using the Coulomb metric, followed by a two-stage pivoted Cholesky decomposition. First, the $(p_a|p_a)$ block is decomposed using a low threshold τ_a, followed by the decomposition of the remaining entries with a higher threshold τ_x. This two-stage procedure guarantees that the proximity of nuclei is well described by functions with high exponents and low angular momentum while expensive functions with high angular momentum are removed to a larger

proportion. The final auxiliary basis is selected from $\{p\}$ according to the obtained pivots. The angular functions of the auxiliary basis set can be chosen to be either solid harmonics or Cartesians.

Forming the complete product space $\{a\} \otimes \{a\}$ in combination with Cartesian angular functions leads to exact results for single atoms by definition, because the product space is fully spanned. This does not hold for systems with more than one atom; here the addition of $\{x\}$ is imperative for accuracy.

The choice of $\{x\}$ depends on the chosen regular basis $\{a\}$. For a double-ζ quality regular basis we found that for complementing the functions with maximum angular momentum $l_{\max}$ an additional function with an exponent of ~ 0.3 is best, while for functions with angular momenta $l_{\max}+1$ and $l_{\max}+2$, exponents of ~ 1.0 recover the most energy in agreement with general rules for basis set construction.[81] If several functions with $l_{\max}+1$ and $l_{\max}+2$ are added, exponents of 1.0 and above are preferable.

For small organic molecules, sub-milli Hartree accuracy can be achieved using a double-ζ regular basis set and an auxiliary basis set which is generated in the described way with one additional diffuse function with angular momenta of $l_{\max}+1$ and $l_{\max}+2$ each relative to the regular basis set. By adding more additional functions and choosing lower Cholesky thresholds, arbitrarily high accuracy can be obtained.

The auxiliary basis set generation is fast and needs to be performed only once. However, $\{x\}$ and τ_x must be chosen carefully to gain any performance advantage over conventional integral-direct techniques.

3.2 Definiteness of ERI tensors

Using benzene as an example system with $R_{\mathrm{CC}} = 1.388\,\text{Å}$ and $R_{\mathrm{CH}} = 1.073\,\text{Å}$, Table 1 lists the smallest eigenvalues of the Mulliken and Dirac ERI matrices in AO basis, thus demonstrating some of the derived bounds (or lack thereof) of Coulomb and exchange energies.

For screened ERIs both error matrices and the Mulliken ERI tensor have negative eigen-

Table 1: Smallest eigenvalues in Hartree (Ha) of the Mulliken and Dirac ERI matrices as well as their respective error matrices ($\Delta(ab|cd) = (ab|cd)_{\text{unscreened}} - (ab|cd)_{\text{screened}}$ in the case of exact integrals and $\Delta(ab|cd) = (ab|cd)_{\text{unscreened}} - \widetilde{(ab|cd)}$ in case of RI approximated integrals (and analogously for $\Delta\langle ab|cd\rangle$).). The underlying system is benzene with cc-pVDZ[82] as regular basis set and either df-def2[77] as auxiliary basis set (RI, PARI) or an automatically generated basis using no additional functions, solid harmonic angular functions, no decontraction, and Cholesky thresholds as given in the table (NRPARI).

	$(ab\|cd)$	$\Delta(ab\|cd)$	$\langle ab\|cd\rangle$	$\Delta\langle ab\|cd\rangle$
screening threshold: 10^{-8} Ha				
exact	-1.182e-08	-5.640e-08	1.697e-08	-1.070e-08
RI	-2.070e-13	-3.461e-08	1.685e-08	-7.155e-03
PARI	-3.432e-02	-3.057e-08	-1.503e-03	-1.073e-02
NRPARI, $\tau_a = 10^{-3}$ Ha	-2.047e-13	-0.2682	-1.807e-02	-7.294e-02
NRPARI, $\tau_a = 10^{-4}$ Ha	-2.047e-13	-0.2682	-1.807e-02	-7.294e-02
NRPARI, $\tau_a = 10^{-6}$ Ha	-2.104e-13	-0.2663	-1.728e-02	-6.926e-02
NRPARI, $\tau_a = 10^{-8}$ Ha	-2.104e-13	-0.2663	-1.728e-02	-6.926e-02
screening threshold: 10^{-12} Ha				
exact	-1.670e-12	-1.787e-11	1.697e-08	-5.799e-12
RI	-2.031e-13	-5.701e-12	1.685e-08	-7.155e-03
PARI	-3.432e-02	-4.508e-12	-1.503e-03	-1.073e-02
NRPARI, $\tau_a = 10^{-3}$ Ha	-2.142e-13	-0.2682	-1.807e-02	-7.294e-02
NRPARI, $\tau_a = 10^{-4}$ Ha	-2.142e-13	-0.2682	-1.807e-02	-7.294e-02
NRPARI, $\tau_a = 10^{-6}$ Ha	-2.157e-13	-0.2663	-1.728e-02	-6.926e-02
NRPARI, $\tau_a = 10^{-8}$ Ha	-2.157e-13	-0.2663	-1.728e-02	-6.926e-02

values which are due to, and can be controlled by, the screening threshold.

In case of global RI, the Mulliken ERI tensor and the associated error matrix have negative eigenvalues which are introduced by screening. The Dirac ERI error matrix has negative eigenvalues which are not directly controlled by the screening threshold.

In the (robust) PARI approximation, the Mulliken ERI tensor is indefinite and the Hartree energy is not bounded from below, which leads to the variational collapse described by Merlot et al.[38] The Mulliken ERI error matrix has negative eigenvalues which are due to screening. The Dirac ERI tensor is indefinite as well, causing the PARI exchange energy to be unbounded from above, which does not impose a problem during SCF optimizations. Despite the Dirac ERI error matrix being indefinite, the exchange energy is bounded from

below as shown in eq. (41).

In the NRPARI approximation very large negative eigenvalues occur in the Mulliken ERI error matrix which are due to large elementwise errors but as it indicates the missing upper bound, this does not impose a problem on SCF optimizations. The indefiniteness of the Dirac ERI tensor does not lead to the absence of an upper bound as shown in eq. (39). Instead, it causes the exchange energy to have no lower bound, an issue that will be investigated in the following.

3.3 RI representations of the Coulomb operator

First we demonstrate the possibility of obtaining negative values of the approximated Coulomb operator in global RI, eq. (23). This potential is shown in Fig. 1 for the CO_2 molecule with $R_{CO} = 1.160\,\text{Å}$, using cc-pVDZ as regular basis set and either df-def2 or automatically generated basis sets as described above (Fig. 1).

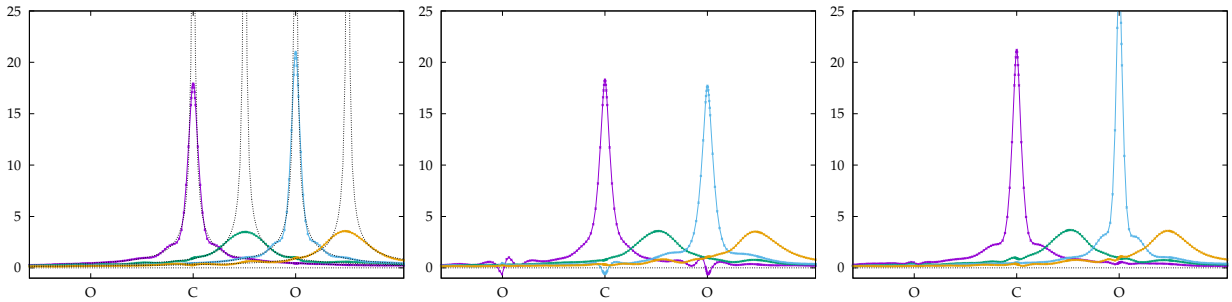

Figure 1: (a) Approximation of the Coulomb operator by global RI using cc-pVDZ/df-def2 plotted along the molecular axis. The first electron is placed at the carbon atom, one oxygen atom, and two arbitrary points on the molecular axis. The ideal r_{12}^{-1} dependence is indicated as a dotted line.; (b) and (c) Approximation of the Coulomb operator by global RI using cc-pVDZ and an auxiliary basis set generated without added functions, solid harmonic angular functions, no decontraction, and Cholesky thresholds b) τ_a of 10^{-4} Ha and c) 10^{-6} Ha.

In the df-def2 reference calculation (Fig. 1(a)), r_{12}^{-1} is reproduced well in the proximity of atoms while the approximation deviates significantly with increasing distance from centers on which basis functions are located. However, the approximated potential is positive

throughout and features the correct r^{-1} long range behavior. Using an auxiliary basis set with a small number of highly contracted orbitals which include high-exponent s-functions, may lead to stabilizing interactions between electrons located close to neighboring nuclei (Fig. 1(b)). This issue vanishes with larger basis sets (Fig. 1(c)), however, this behavior is hard to predict.

As predicted (eq. (39)) the issue of obtaining negative values for the Coulomb operator and hence negative ERI eigenvalues also applies to nonrobust local RI which is demonstrated at the example of NRPARI. In the nonrobust local RI approximation, r_{12}^{-1} is approximated as

$$r_{12}^{-1} \approx \sum_{\alpha\beta\gamma\delta} \int \frac{\alpha(\boldsymbol{r}')}{|\boldsymbol{r}_1 - \boldsymbol{r}'|} \mathrm{d}\boldsymbol{r}' (\alpha|\beta)^{-1} (\beta|\gamma)(\gamma|\delta)^{-1} \int \frac{\delta(\boldsymbol{r}')}{|\boldsymbol{r}_2 - \boldsymbol{r}'|} \mathrm{d}\boldsymbol{r}' \tag{43}$$

for an integral $(ab|cd)$ where functions α and β are located on the same centers as a and b, and γ and δ are located on the centers of c and d.

Using CO_2 and benzene as test systems, negative values for the Coulomb operator are found for the integrals of type $(ab|ab)$ where a and b are located on neighboring second row atoms (Figs. 2 and 3). They are located close to but not always on atomic centers. Not unexpectedly, the electron repulsion is poorly described at large distances from either of the two centers on which the product is expanded.

3.4 Variational instabilities in SCF optimizations

Even though stabilizing electron-electron interactions are confined to small spatial domains, the SCF optimizer may amass extremely high electron density in them, leading to largly negative exchange energies and hence very low total energies. This problem is aggravated by the fact that electron density in close proximity to nuclei is further stabilized by nuclear-electronic attraction. Fig. 4 visualizes how, during the HF optimization of benzene, unphysically low energies result from extremely large off-diagonal entries in the density which correspond to near-orthogonal atomic orbitals. These high densities can be monitored through the eigen-

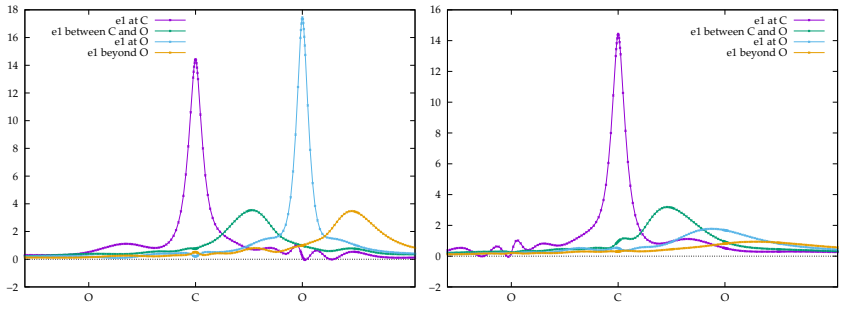

Figure 2: Coulomb operator in the nonrobust local RI approximation (eq. (43)) for the integrals $(ab|ab)$ where a and b are located on (a) the carbon atom and the right oxygen atom, and (b) the carbon atom and the left oxygen atom. The regular basis set is cc-pVDZ and the auxiliary basis set was generated as described above without added functions, without decontraction, solid harmonic angular functions, and a Cholesky threshold of 10^{-3} Ha. The plotted coordinates lie on the molecular axis.

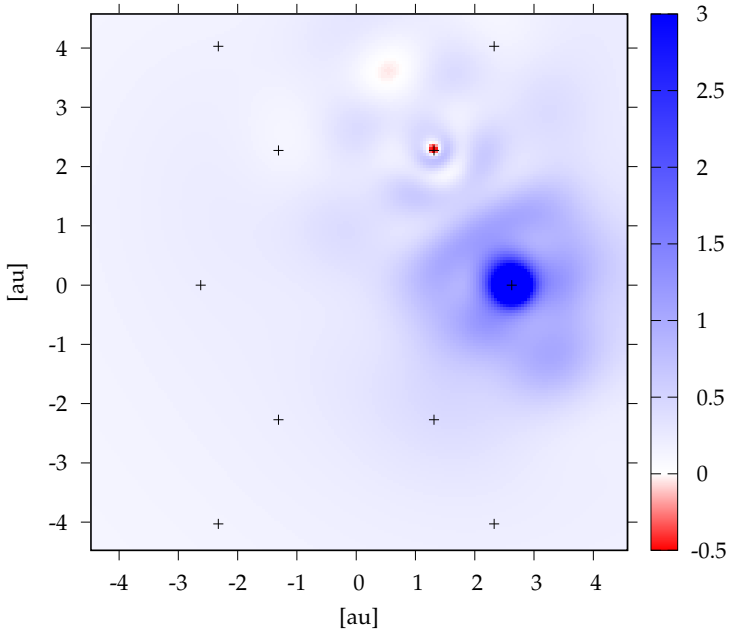

Figure 3: Coulomb operator in the nonrobust local RI approximation (eq. (43)) for the integral $(ab|ab)$ where a and b are located on two neighboring carbon atoms in benzene. The regular basis set is cc-pVDZ and the auxiliary basis set was generated as described above without added functions, without decontraction, solid harmonic angular functions, and a Cholesky threshold of 10^{-3} Ha. The plot lies in the molecular plane; positions of atoms are indicated as '+'.

values of the density matrix. In all of the following calculations the density is optimized using the Roothaan-Hall scheme in combination with DIIS.

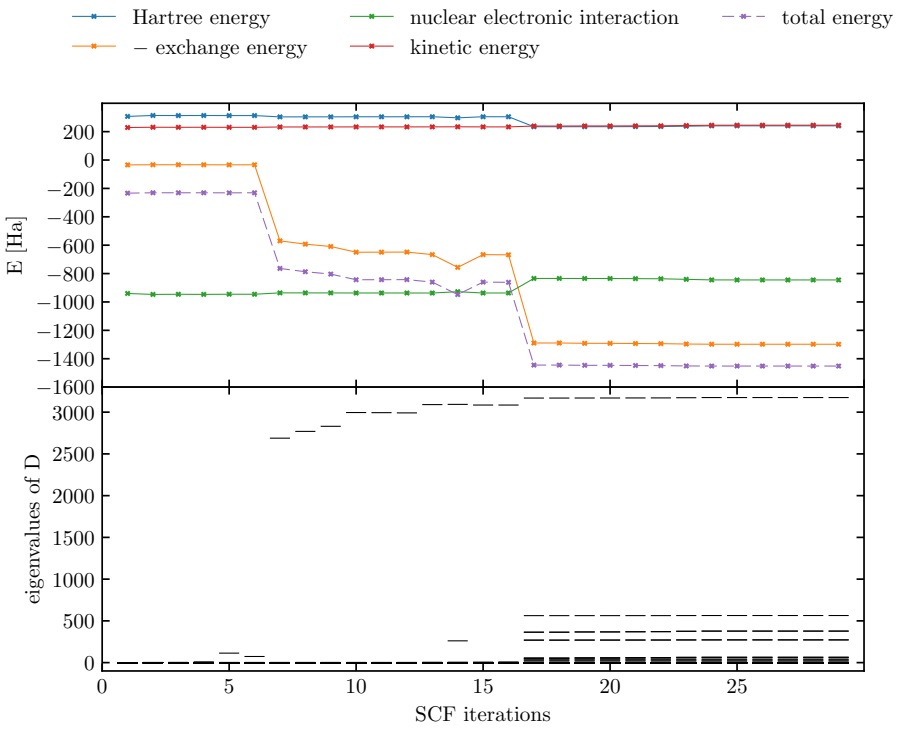

Figure 4: Energy contributions during the HF optimization of benzene using NRPARI with cc-pVDZ as a regular basis set and an auxiliary basis set generated without added functions, with solid harmonic angular functions, no decontraction, and a Cholesky threshold of $3 \cdot 10^{-3}$. The second subplot depicts the eigenvalues of the one-electron density matrix which clearly correspond to the above energy plot.

While negative values of the approximated Coulomb potential are clearly unphysical, their presence need not in every case lead to unphysical electronic states. As an example, neither of the carbon dioxide calculations for which the Coulomb operators are plotted above show variational instabilities and do not lead to unphysically low exchange energies.

These physically correct states which are obtained in the presence of stabilizing electron–electron interactions make it even harder to predict when calculations will fail, and hence, how far the size of the auxiliary basis set may be reduced. As Fig. 5 shows, removal of functions from the auxiliary basis set through an increased τ_a does not lead to a gradual but rather to a sudden decay. The same auxiliary basis set may lead to unphysical states

for some molecules while the SCF optimization still converges to the physical state for other molecules of comparable size and with similar structural features. The Cholesky threshold $\tau_a = 3 \cdot 10^{-3}$ Ha at which the variational breakdown occurs is not an unrealistic choice, taking into account the inherent basis set incompleteness error of cc-pVDZ, which is estimated to be 75 mHa by comparison with the accurate pcseg-4 basis set of Jensen.[83,84] Moreover, no significant error reduction is observed for similar molecules by lowering τ_a. More accuracy would be achieved by augmentation in the auxiliary basis set generation, but this increases the computational cost significantly.

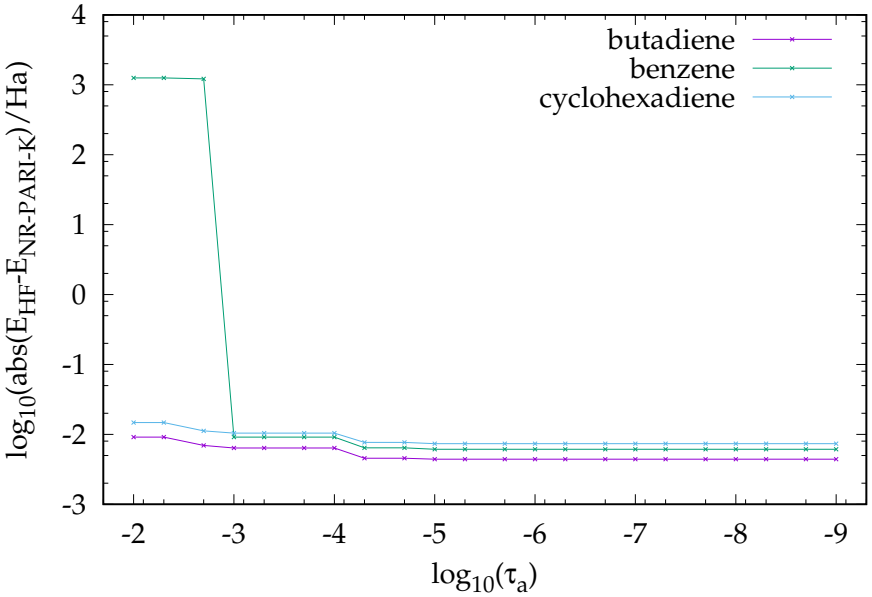

Figure 5: Energy errors of HF/NRPARI-K compared to exact HF of butadiene, benzene, and cyclohexadiene. Using cc-pVDZ as regular basis set, no added functions and varying Cholesky thresholds during the basis set generation.

As a second example, we look at a series of HF/NRPARI-K energies of a benzene molecule with the same geometry as above; the regular basis sets are pcseg-1, pcseg-2, and pcseg-3,[83] and the auxiliary basis sets are automatically generated with no additional functions $\{x\}$, and a Cholesky threshold $\tau_a = 10^{-7}$ Ha. The energy errors of the converged NRPARI-K calculations relative to the exact energies of the respective converged electron densities are +7.91 mHa for pcseg-1, +0.46 mHa for pcseg-2, and $-2,699,554,500$ mHa for pcseg-3. Somewhat surprisingly, the NRPARI-K/pcseg-3 calculation converges in just 6 cycles. For

the first two basis sets, pcseg-1 and pcseg-2, these errors are utterly negligible compared with the basis set incompleteness errors of 157 mHa and 25.6 mHa, respectively, as estimated relative to pcseg-4. The estimated basis set error of pcseg-3 is just 3.3 mHa. This example clearly demonstrates that even for low Cholesky thresholds corresponding to errors that are acceptable for production calculations, convergence to unphysical states cannot be ruled out.

4 Conclusions

We have presented a theoretical analysis of the variational stability of global and local RI approximations by examining the definiteness of the Mulliken and Dirac ERI matrices. For general trial wave functions, neither global nor local RI approximations guarantee variational stability. For the important special case of a single determinant wave function, the global RI approximation may produce negative electron–electron repulsion energies but since both the Hartree and exchange contributions are bounded from below, variational stability is guaranteed. Unfortunately, this property is not conserved within local RI approximations. Within robust local RI approximations, the Hartree contribution is unbounded from below whereas the exchange contribution is bounded from below. Conversely, within nonrobust local RI approximations, the Hartree contribution is bounded from below whereas the exchange contribution is unbounded from below. Table 2 summarizes ERI matrix properties and lower

Table 2: Summary of results on positive definiteness of ERI matrices and on the existence of lower bounds of single-determinant energy contributions. Lack of lower bounds implies that variational stability is not guaranteed.

	ERI matrix positive semidefinite?		Energy contribution bounded from below?	
	Mulliken	Dirac	Hartree	Exchange
Exact	Yes	Yes	Yes	Yes
RI	Yes	No	Yes	Yes
Robust local RI	No	No	No	Yes
Nonrobust local RI	Yes	No	Yes	No

bounds (or lack thereof) of RI, robust local RI, and nonrobust local RI relative to the exact Hartree and exchange energies for a given single-determinant state. The theoretical findings are illustrated by calculations on two simple molecules, CO_2 and benzene.

The variational stability problems can be alleviated by using a sufficiently flexible auxiliary basis set, thus trading efficiency for accuracy. We have adapted an automated auxiliary basis set generation scheme proposed by Ihrig et al.[43] for numerical basis functions to Gaussian-type orbitals, aiming at improved accuracy of the nonrobust PARI approximation in particular. Very large auxiliary basis sets are required to achieve satisfactory accuracy and the methodology, in its present formulation, is not competitive. The more commonly used local domain fitting is an alternative approach to obtaining sufficient accuracy. In addition to the well-known continuity problems associated with this approach, our analysis shows that one can not generally determine the smallest domain size at which variational collapse is avoided. In the end, the only safe approach would be to use nonrobust local (or global) RI for the Hartree contribution and robust local RI for the exchange contribution. In particular, we note that nonhybrid Kohn-Sham density-functional theory (KS-DFT) calculations should avoid robust local RI approximations.

Finally, we note that the tensor hypercontraction (THC) scheme developed by Martínez and coworkers[53–55,57–62,64–66] is based on either global or local RI and thus inherits the properties of the parent RI approximation as summarized in Table 2. Since the THC approximation is not competitive for single determinant optimizations and instead is applied to nonvariational electron correlation models (Møller-Plesset perturbation theory and coupled-cluster theory), variational instability issues are not a major concern at present.

Acknowledgement

This work has been supported by the Research Council of Norway (RCN) through a Centre of Excellence Grant (Grant No. 179568/V30) and through the RCN Research Grant No.

240698/F20. This work has received support from the Norwegian Supercomputing Program (NOTUR) through a grant of computer time (Grant No. NN4654K).

References

(1) Yserentant, H. In *Regularity and Approximability of Electronic Wave Functions*; Morel, J.-M., Takens, F., Teissier, B., Eds.; Lecture Notes in Mathematics; Springer: Berlin, Heidelberg, 2010; Vol. 2000.

(2) Häser, M.; Ahlrichs, R. Improvements on the direct SCF method. *J. Comput. Chem.* **1989**, *10*, 104–111.

(3) Ochsenfeld, C.; White, C. A.; Head-Gordon, M. Linear and sublinear scaling formation of Hartree-Fock-type exchange matrices. *J. Chem. Phys.* **1998**, *109*, 1663–1669.

(4) Lambrecht, D. S.; Ochsenfeld, C. Multipole-based integral estimates for the rigorous description of distance dependence in two-electron integrals. *J. Chem. Phys.* **2005**, *123*, 184101.

(5) Lambrecht, D. S.; Doser, B.; Ochsenfeld, C. Rigorous integral screening for electron correlation methods. *J. Chem. Phys.* **2005**, *123*, 184102.

(6) Doser, B.; Lambrecht, D. S.; Ochsenfeld, C. Tighter multipole-based integral estimates and parallel implementation of linear-scaling AO-MP2 theory. *Phys. Chem. Chem. Phys.* **2008**, *10*, 3335–3344.

(7) Maurer, S. A.; Lambrecht, D. S.; Flaig, D.; Ochsenfeld, C. Distance-dependent Schwarz-based integral estimates for two-electron integrals: reliable tightness vs. rigorous upper bounds. *J. Chem. Phys.* **2012**, *136*, 144107.

(8) Boys, S. F.; Shavitt, I. *A Fundamental Calculation of the Energy Surface for the System of Three Hydrogen Atoms*; University of Wisconsin Technical Report WIS-AF-13, 1959.

(9) Whitten, J. L. Coulombic potential energy integrals and approximations. *J. Chem. Phys.* **1973**, *58*, 4496–4501.

(10) Baerends, E.; Ellis, D.; Ros, P. Self-consistent molecular Hartree-Fock-Slater calculations I. The computational procedure. *Chem. Phys.* **1973**, *2*, 41–51.

(11) Sambe, H.; Felton, R. H. A new computational approach to Slater's SCF-Xα equation. *J. Chem. Phys.* **1975**, *62*, 1122–1126.

(12) Beebe, N. H. F.; Linderberg, J. Simplifications in the generation and transformation of two-electron integrals in molecular calculations. *Int. J. Quantum Chem.* **1977**, *12*, 683–705.

(13) Dunlap, B. I.; Connolly, J. W. D.; Sabin, J. R. On some approximations in applications of Xα theory. *J. Chem. Phys.* **1979**, *71*, 3396–3402.

(14) Dunlap, B. I.; Connolly, J. W. D.; Sabin, J. R. On first-row diatomic molecules and local density models. *J. Chem. Phys.* **1979**, *71*, 4993–4999.

(15) Feyereisen, M.; Fitzgerald, G.; Komornicki, A. Use of approximate integrals in ab initio theory. An application in MP2 energy calculations. *Chem. Phys. Lett.* **1993**, *208*, 359–363.

(16) Vahtras, O.; Almlöf, J.; Feyereisen, M. Integral approximations for LCAO-SCF calculations. *Chem. Phys. Lett.* **1993**, *213*, 514–518.

(17) Gallant, R. T.; St-Amant, A. Linear scaling for the charge density fitting procedure of the linear combination of Gaussian-type orbitals density functional method. *Chem. Phys. Lett.* **1996**, *256*, 569–574.

(18) Fonseca Guerra, C.; Snijders, J. G.; te Velde, G.; Baerends, E. J. Towards an order-N DFT method. *Theor. Chem. Acc.* **1998**, *99*, 391–403.

(19) Dunlap, B. I. Robust variational fitting: Gáspár's variational exchange can accurately be treated analytically. *J. Mol. Struct. (THEOCHEM)* **2000**, *501–502*, 221–228.

(20) Dunlap, B. I. Robust and variational fitting: Removing the four-center integrals from center stage in quantum chemistry. *J. Mol. Struct. (THEOCHEM)* **2000**, *529*, 37–40.

(21) Dunlap, B. I. Robust and variational fitting. *Phys. Chem. Chem. Phys.* **2000**, *2*, 2113–2116.

(22) Weigend, F. A fully direct RI-HF algorithm: Implementation, optimised auxiliary basis sets, demonstration of accuracy and efficiency. *Phys. Chem. Chem. Phys.* **2002**, *4*, 4285–4291.

(23) Koch, H.; Sánchez de Merás, A.; Pedersen, T. B. Reduced scaling in electronic structure calculations using Cholesky decompositions. *J. Chem. Phys.* **2003**, *118*, 9481–9484.

(24) Sierka, M.; Hogekamp, A.; Ahlrichs, R. Fast evaluation of the Coulomb potential for electron densities using multipole accelerated resolution of identity approximation. *J. Chem. Phys.* **2003**, *118*, 9136–9148.

(25) Polly, R.; Werner, H.-J.; Manby, F. R.; Knowles, P. J. Fast Hartree-Fock theory using local density fitting approximations. *Mol. Phys.* **2004**, *102*, 2311–2321.

(26) Jung, Y.; Sodt, A.; Gill, P. M. W.; Head-Gordon, M. Auxiliary basis expansions for large-scale electronic structure calculations. *Proc. Natl. Acad. Sci. USA* **2005**, *102*, 6692–6697.

(27) Gill, P. M. W.; Gilbert, A. T. B.; Taylor, S. W.; Friesecke, G.; Head-Gordon, M. Decay behavior of least-squares coefficients in auxiliary basis expansions. *J. Chem. Phys.* **2005**, *123*, 61101.

(28) Sodt, A.; Subotnik, J. E.; Head-Gordon, M. Linear scaling density fitting. *J. Chem. Phys.* **2006**, *125*, 194109.

(29) Aquilante, F.; Pedersen, T. B.; Lindh, R. Low-cost evaluation of the exchange Fock matrix from Cholesky and density fitting representations of the electron repulsion integrals. *J. Chem. Phys.* **2007**, *126*, 194106.

(30) Sałek, P.; Høst, S.; Thøgersen, L.; Jørgensen, P.; Manninen, P.; Olsen, J.; Jansík, B.; Reine, S.; Pawłowski, F.; Tellgren, E.; Helgaker, T.; Coriani, S. Linear-scaling implementation of molecular electronic self-consistent field theory. *J. Chem. Phys.* **2007**, *126*, 114110.

(31) Reine, S.; Tellgren, E.; Krapp, A.; Kjærgaard, T.; Helgaker, T.; Jansík, B.; Høst, S.; Sałek, P. Variational and robust density fitting of four-center two-electron integrals in local metrics. *J. Chem. Phys.* **2008**, *129*, 104101.

(32) Sodt, A.; Head-Gordon, M. Hartree-Fock exchange computed using the atomic resolution of the identity approximation. *J. Chem. Phys.* **2008**, *128*, 104106.

(33) Pedersen, T. B.; Aquilante, F.; Lindh, R. Density fitting with auxiliary basis sets from Cholesky decompositions. *Theor. Chem. Acc.* **2009**, *124*, 1–10.

(34) Köster, A. M.; del Campo, J. M.; Janetzko, F.; Zuniga-Gutierrez, B. A MinMax self-consistent-field approach for auxiliary density functional theory. *J. Chem. Phys.* **2009**, *130*, 114106.

(35) Domínguez-Soria, V. D.; Geudtner, G.; Morales, J. L.; Calaminici, P.; Köster, A. M. Robust and efficient density fitting. *J. Chem. Phys.* **2009**, *131*, 124102.

(36) Burow, A. M.; Sierka, M.; Mohamed, F. Resolution of identity approximation for the Coulomb term in molecular and periodic systems. *J. Chem. Phys.* **2009**, *131*, 214101.

(37) Dunlap, B. I.; Rösch, N.; Trickey, S. B. Variational fitting methods for electronic structure calculations. *Mol. Phys.* **2010**, *108*, 3167–3180.

(38) Merlot, P.; Kjærgaard, T.; Helgaker, T.; Lindh, R.; Aquilante, F.; Reine, S.; Pedersen, T. B. Attractive electron-electron interactions within robust local fitting approximations. *J. Comput. Chem.* **2013**, *34*, 1486–1496.

(39) Mejía-Rodríguez, D.; Köster, A. M. Robust and efficient variational fitting of Fock exchange. *J. Chem. Phys.* **2014**, *141*, 124114.

(40) Hollman, D. S.; Schaefer, H. F.; Valeev, E. F. Semi-exact concentric atomic density fitting: Reduced cost and increased accuracy compared to standard density fitting. *J. Chem. Phys.* **2014**, *140*, 064109.

(41) Manzer, S. F.; Epifanovsky, E.; Head-Gordon, M. Efficient Implementation of the Pair Atomic Resolution of the Identity Approximation for Exact Exchange for Hybrid and Range-Separated Density Functionals. *J. Chem. Theory Comput.* **2015**, *11*, 518–527.

(42) Manzer, S.; Horn, P. R.; Mardirossian, N.; Head-Gordon, M. Fast, accurate evaluation of exact exchange: The occ-RI-K algorithm. *J. Chem. Phys.* **2015**, *143*, 024113.

(43) Ihrig, A. C.; Wieferink, J.; Zhang, I. Y.; Ropo, M.; Ren, X.; Rinke, P.; Scheffler, M.; Blum, V. Accurate localized resolution of identity approach for linear-scaling hybrid density functionals and for many-body perturbation theory. *New J. Phys.* **2015**, *17*, 093020.

(44) Golze, D.; Iannuzzi, M.; Hutter, J. Local Fitting of the Kohn-Sham Density in a Gaussian and Plane Waves Scheme for Large-Scale Density Functional Theory Simulations. *J. Chem. Theory Comput.* **2017**, *13*, 2202–2214.

(45) Friesner, R. A. Solution of self-consistent field electronic structure equations by a pseudospectral method. *Chem. Phys. Lett.* **1985**, *116*, 39–43.

(46) Friesner, R. A. Solution of the Hartree-Fock equations by a pseudospectral method: Application to diatomic molecules. *J. Chem. Phys.* **1986**, *85*, 1462–1468.

(47) Friesner, R. A. Solution of the Hartree-Fock equations for polyatomic molecules by a pseudospectral method. *J. Chem. Phys.* **1987**, *86*, 3522–3531.

(48) Martínez, T. J.; Carter, E. A. In *Modern Electronic Structure Theory*; Yarkony, D. R., Ed.; World Scientific: Singapore, 1995; pp 1132–1165.

(49) Neese, F.; Wennmohs, F.; Hansen, A.; Becker, U. Efficient, approximate and parallel Hartree-Fock and hybrid DFT calculations. A 'chain-of-spheres' algorithm for the Hartree-Fock exchange. *Chem. Phys.* **2009**, *356*, 98–109.

(50) Izsák, R.; Neese, F. An overlap fitted chain of spheres exchange method. *J. Chem. Phys.* **2011**, *135*, 144105.

(51) Izsák, R.; Neese, F.; Klopper, W. Robust fitting techniques in the chain of spheres approximation to the Fock exchange: The role of the complementary space. *J. Chem. Phys.* **2013**, *139*, 094111.

(52) Benedikt, U.; Auer, A. A.; Espig, M.; Hackbusch, W. Tensor decomposition in post-Hartree-Fock methods. I. Two-electron integrals and MP2. *J. Chem. Phys.* **2011**, *134*, 054118.

(53) Hohenstein, E. G.; Parrish, R. M.; Martínez, T. J. Tensor hypercontraction density fitting. I. Quartic scaling second- and third-order Møller-Plesset perturbation theory. *J. Chem. Phys.* **2012**, *137*, 044103.

(54) Parrish, R. M.; Hohenstein, E. G.; Martínez, T. J.; Sherrill, C. D. Tensor hypercontraction. II. Least-squares renormalization. *J. Chem. Phys.* **2012**, *137*, 224106.

(55) Hohenstein, E. G.; Parrish, R. M.; Sherrill, C. D.; Martínez, T. J. Communication: Tensor hypercontraction. III. Least-squares tensor hypercontraction for the determination of correlated wavefunctions. *J. Chem. Phys.* **2012**, *137*, 221101.

(56) Benedikt, U.; Böhm, K.-H.; Auer, A. A. Tensor decomposition in post-Hartree-Fock methods. II. CCD implementation. *J. Chem. Phys.* **2013**, *139*, 224101.

(57) Parrish, R. M.; Hohenstein, E. G.; Martínez, T. J.; Sherrill, C. D. Discrete variable representation in electronic structure theory: Quadrature grids for least-squares tensor hypercontraction. *J. Chem. Phys.* **2013**, *138*, 194107.

(58) Hohenstein, E. G.; Kokkila, S. I. L.; Parrish, R. M.; Martínez, T. J. Quartic scaling second-order approximate coupled cluster singles and doubles via tensor hypercontraction: THC-CC2. *J. Chem. Phys.* **2013**, *138*, 124111.

(59) Hohenstein, E. G.; Kokkila, S. I. L.; Parrish, R. M.; Martínez, T. J. Tensor Hypercontraction Equation-of-Motion Second-Order Approximate Coupled Cluster: Electronic Excitation Energies in Time. *J. Phys. Chem. B* **2013**, *117*, 12972–12978.

(60) Parrish, R. M.; Hohenstein, E. G.; Schunck, N. F.; Sherrill, C. D.; Martínez, T. J. Exact Tensor Hypercontraction: A Universal Technique for the Resolution of Matrix Elements of Local Finite-Range N -Body Potentials in Many-Body Quantum Problems. *Phys. Rev. Lett.* **2013**, *111*, 132505.

(61) Parrish, R. M.; Sherrill, C. D.; Hohenstein, E. G.; Kokkila, S. I. L.; Martínez, T. J. Communication: Acceleration of coupled cluster singles and doubles via orbital-weighted least-squares tensor hypercontraction. *J. Chem. Phys.* **2014**, *140*, 181102.

(62) Lu, J.; Ying, L. Compression of the electron repulsion integral tensor in tensor hypercontraction format with cubic scaling cost. *J. Comput. Phys.* **2015**, *302*, 329–335.

(63) Hoy, E. P.; Mazziotti, D. A. Positive semidefinite tensor factorizations of the two-electron integral matrix for low-scaling ab initio electronic structure. *J. Chem. Phys.* **2015**, *143*, 064103.

(64) Parrish, R. M.; Hohenstein, E. G.; Martínez, T. J. Comment on 'Positive semidefinite tensor factorizations of the two-electron integral matrix for low-scaling ab initio electronic structure' [J. Chem. Phys. 143, 064103 (2015)]. *J. Chem. Phys.* **2016**, *145*, 027101.

(65) Song, C.; Martínez, T. J. Atomic orbital-based SOS-MP2 with tensor hypercontraction. I. GPU-based tensor construction and exploiting sparsity. *J. Chem. Phys.* **2016**, *144*, 174111.

(66) Song, C.; Martínez, T. J. Atomic orbital-based SOS-MP2 with tensor hypercontraction. II. Local tensor hypercontraction. *J. Chem. Phys.* **2017**, *146*, 034104.

(67) Billingsley, F. P.; Bloor, J. E. Limited Expansion of Diatomic Overlap (LEDO): A Near-Accurate Approximate Ab Initio LCAO MO Method. I. Theory and Preliminary Investigations. *J. Chem. Phys.* **1971**, *55*, 5178–5190.

(68) Aquilante, F.; Lindh, R.; Pedersen, T. B. Unbiased auxiliary basis sets for accurate two-electron integral approximations. *J. Chem. Phys.* **2007**, *127*, 114107.

(69) Aquilante, F.; Gagliardi, L.; Pedersen, T. B.; Lindh, R. Atomic Cholesky decompositions: A route to unbiased auxiliary basis sets for density fitting approximation with tunable accuracy and efficiency. *J. Chem. Phys.* **2009**, *130*, 154107.

(70) Helgaker, T.; Jørgensen, P.; Olsen, J. *Molecular Electronic-Structure Theory*; John Wiley and Sons, Ltd: Chichester, 2000.

(71) Slater, J. C. *Quantum Theory of Atomic Structure, Vol. I*; McGraw-Hill: New York, 1960; (Appendix 19).

(72) Roothaan, C. C. J. New Developments in Molecular Orbital Theory. *Rev. Mod. Phys.* **1951**, *23*, 69–89.

(73) Power, J. D.; Pitzer, R. M. Inequalities For Electron Repulsion Integrals. *Chem. Phys. Lett.* **1974**, *24*, 478–483.

(74) Manby, F. R.; Knowles, P. J. Poisson Equation in the Kohn-Sham Coulomb Problem. *Phys. Rev. Lett.* **2001**, *87*, 163001.

(75) Aquilante, F.; Pedersen, T. B.; Sánchez de Merás, A.; Koch, H. Fast noniterative orbital localization for large molecules. *J. Chem. Phys.* **2006**, *125*, 174101.

(76) Weigend, F. Accurate Coulomb-fitting basis sets for H to Rn. *Phys. Chem. Chem. Phys.* **2006**, *8*, 1057–1065.

(77) Weigend, F. Hartree-Fock exchange fitting basis sets for H to Rn. *J. Comput. Chem.* **2008**, *29*, 167–175.

(78) Boström, J.; Aquilante, F.; Pedersen, T. B.; Lindh, R. *Ab Initio* Density Fitting: Accuracy Assessment of Auxiliary Basis Sets from Cholesky Decompositions. *J. Chem. Theory Comput.* **2009**, *5*, 1545–1553.

(79) Boström, J.; Delcey, M. G.; Aquilante, F.; Serrano-Andrés, L.; Pedersen, T. B.; Lindh, R. Calibration of Cholesky Auxiliary Basis Sets for Multiconfigurational Perturbation Theory Calculations of Excitation Energies. *J. Chem. Theory Comput.* **2010**, *6*, 747–754.

(80) Boström, J.; Pitoňák, M.; Aquilante, F.; Neogrády, P.; Pedersen, T. B.; Lindh, R. Coupled Cluster and Møller-Plesset Perturbation Theory Calculations of Noncovalent Intermolecular Interactions using Density Fitting with Auxiliary Basis Sets from Cholesky Decompositions. *J. Chem. Theory Comput.* **2012**, *8*, 1921–1928.

(81) Nagy, B.; Jensen, F. Basis sets in Quantum Chemistry. *Rev. Comput. Chem.* **2017**, *30*, 93–149.

(82) Dunning, Jr., T. H. Gaussian basis sets for use in correlated molecular calculations. I. The atoms boron through neon and hydrogen. *J. Chem. Phys.* **1989**, *90*, 1007–1023.

(83) Jensen, F. Unifying General and Segmented Contracted Basis Sets. Segmented Polarization Consistent Basis Sets. *J. Chem. Theory Comput.* **2014**, *10*, 1074–1085.

(84) Jensen, F. How Large is the Elephant in the Density Functional Theory Room? *J. Phys. Chem. A* **2017**, *121*, 6104–6107.